4. Applied Methods

Traditionally, a battery of bioanalytical and biophysical techniques that range from high resolution methods such as NMR and X-ray crystallography to low resolution methods like CD and FTIR spectroscopy, are applied for the characterization of fibril forming proteins *in vitro*. Depending on the underlying physical and chemical principles, these methods provide distinctly different information on structure and formation kinetics of amyloids. In order to appraise their capabilities correctly, this section will briefly summarize and describe the analytical techniques applied here. Further information on the particular method can be obtained from the cited literature.
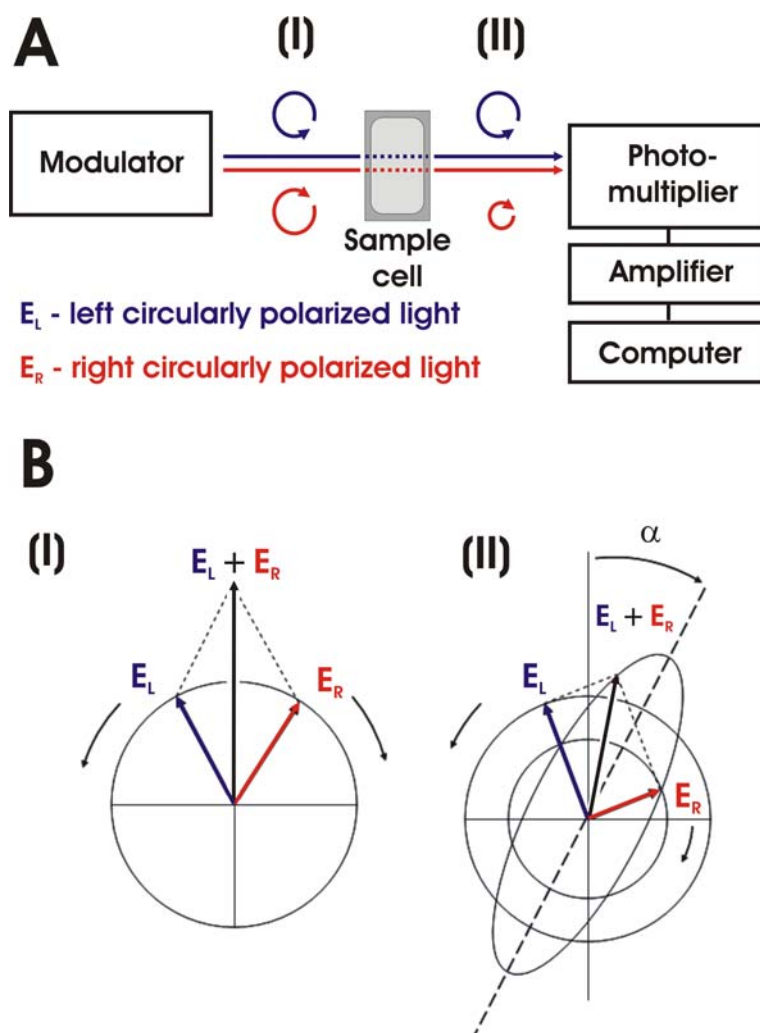
4.1 Circular Dichroism (CD) Spectroscopy

Circular dichroism spectroscopy provides a low-resolution picture of the protein conformation and is one of the most widely used techniques for the characterization of peptides and proteins in solution.[166,167] The instrumentation is very well established, robust and commercially available. Furthermore, it is non-destructive and not very demanding in terms of sample workup and consumption, thus enabling an application on a routine basis. During the work on this thesis, CD spectroscopy was used as a standard method to follow conformational transitions of the designed peptides.

4.1.1 Physical Principles

Like FTIR spectroscopy, CD spectroscopy provides cumulative information on the structural distribution of biomolecules. The underlying physical principle is the varying, wavelength dependent absorption of left and right circularly polarized light by chromophores in chiral molecules. Besides glycine, which is not optically active, peptides and proteins exclusively consist of enantiomeric amino acids and are therefore highly suitable for characterization by CD spectroscopy. Moreover, all amino acids are connected by peptide bonds, which represent the most ubiquitous chromophore in peptides and proteins. This yields two characteristic absorption bands in the far-UV region (λ = 190-250nm): a π-π* transition at 190nm and a weaker and broader n-π* transition at 210nm.[166] Different types of secondary structure arrange the peptide bonds in a spe-

cific asymmetric, non-random fashion, giving rise to characteristic CD spectra in this wavelength range.

Figure 4.1 shows instrumentation and working principles of a CD spectrometer. For a better comprehensibility, a two beam setup is described here (Figure 4.1 A), although modern instruments are usually one beam devices. Two beams of monochromatic left and right circularly polarized light are provided by phase modulation of monochromatic, linearly polarized light in the modulator. These beams are traversing the sample that, following Lambert-Beer's law, absorbs light from both components to a different extend. Subsequently, both beams are detected by a photomultiplier, amplified, and recorded by a computer workstation.

Figure 4.1. *Instrumentation and working principle of circular dichroism. (A) Schematic chart of a two-beam CD spectrometer. (B) Field vectors of left (blue) and right (red) circularly polarized light and their superposition (black), before (I) and after (II) passage through the sample.*

The physics of circular dichroism can be explained more precisely by the field vectors of the circularly polarized components. A very clear and detailed explanation using computer animated models is described elsewere.[168] Figure 4.1 B shows the field vectors of left (blue) and right (red) circularly polarized light and their superposition (black), before (I) and after (II) traversing the sample. An in-phase combination of left (E_L) and right (E_R) circularly polarized light with equal amplitude and wavelength yields plane polarized light. Thus, the superposition of both beams results in a simple line (Figure 4.1 (I)). This is the case in a CD spectrometer before the beam passes through the sample. In contrast, traverse through an asymmetric sample results in a differing absorption of the circularly polarized beams. The consequence is that a projection of the resulting amplitude now yields an ellipse instead of a line (Figure 4.1 (II)). The occurrence of this ellipse is called *circular dichroism*. Additionally, rotation of the polarization plane, i.e., the axes of the dichroic ellipse, by a small angle α occurs when the phases of the two circularly polarized components become different. This optical rotation effect is caused by differing propagation velocities, i.e., refractive indices and is therefore called circular birefringence. Circular dichroism and optical rotation are directly related and therefore occur simultaneously.[166,168]

4.1.2 Data Analysis

Although modern instruments directly measure the difference in absorption ΔA, for historical reasons the circular dichroism is usually expressed in degrees of ellipticity [θ]. The following section should briefly point out the connection between these two parameters. The full derivation can be obtained from the literature.[166] At a given wavelength, the difference of the absorptions of left (A_L) and right (A_R) polarized light can be expressed as:

$$\Delta A = A_L - A_R \tag{1}$$

applying Lambert-Beer's law yields:

$$\Delta A = (\varepsilon_L + \varepsilon_R)dc = \Delta \varepsilon dc \tag{2}$$

with path length d [cm], concentration c [mol/L], and the molar extinction coefficients of left and right circular polarized light ε_L and ε_R. The resulting, path length and concentration independent Δε is the circular dichroism.

On the other hand, the ellipticity of the polarization θ is originated from the magnitudes of the electric field vectors E_L and E_R using the rules of trigonometry. These field vectors can be substituted by the square root of the intensity of irradiation of the left and right circular polarized light. This enables the application of Lambert-Beer's law, yielding a complex equation that can be solved utilizing a Taylor series. The resulting equation of θ in degrees is:

$$\theta = \Delta A(\frac{\ln 10}{4})(\frac{180}{\pi}) \tag{3}$$

The dependence of θ on path length and concentration can be removed defining the molar ellipticity $[\theta]$ as:

$$[\theta] = \frac{100\theta}{dc} \tag{4}$$

Combining (3) and (4) and (2) yields the multiplicative relation between the circular dichroism $\Delta\varepsilon$ and the molar ellipticity.

$$[\theta] = 100\Delta\varepsilon(\frac{\ln 10}{4})(\frac{180}{\pi}) = 3298.2\Delta\varepsilon \tag{5}$$

For practical reasons and in order to compare the absolute intensity of proteins with a differing number of amino acids, spectra are usually given in mean residue ellipticity:

$$[\theta]_{mr} = \frac{[\theta]100M}{cdN} \tag{6}$$

where M is the molar weight [g/mol], c the concentration [mg/mL], d the path length [cm] and N the number of amino acids. All CD spectra shown in this thesis are given in molar ellipticity per residue which was calculated using equation (6).

4.1.3 Protein Structure Determination

Far-UV spectra of peptides and proteins can be used to predict characteristics of their secondary structure. This is based on the fact that isolated α-helices, β-sheets, and random coils possess characteristic, distinctly different signatures. However, the princi-

ples leading to these signatures are theoretically not understood yet. The first basis CD spectra obtained from the different, pH dependent conformations of poly-L-lysine were reported by G.D. Fasman et al.[169] Today, other proteins, such as myloglobin, (Lys-Leu)$_n$, and (Pro-Lys-Leu-Lys-Leu)$_n$ are used as standards for α-helices, β-sheets, and random coils, respectively.[170] Small peptides with defined conformation have also been applied.[171] Figure 4.2 shows far-UV CD signatures of β-sheets, α-helices, and random coils measured in our lab.
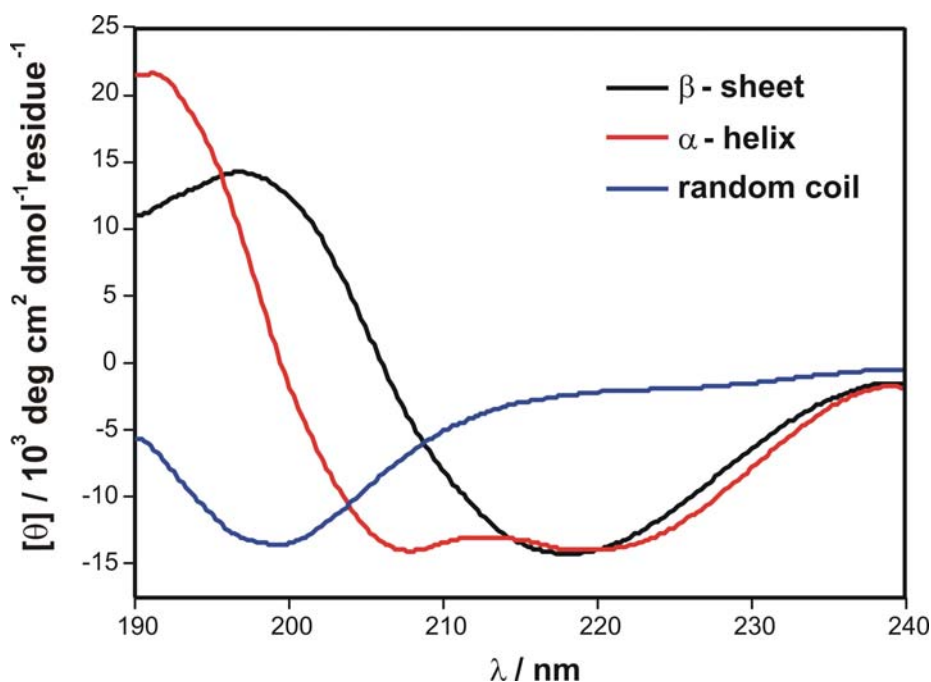
Figure 4.2. *Characteristic far-UV spectra of β-sheets (black), α-helices (red), and random coils (blue). Typical bands are: β-sheet - negative at 216nm (π-π*), positive at 195-198nm (n-π*); α-helix – positive at 192-195nm (π–π*), negative at 208nm (π–π*) and 222nm (n-π*); random coil - negative at 200nm (n-π*).*

The secondary structure composition of a complex protein's globular fold can be determined utilizing these idealized basis spectra in the following equation:

$$CD_{Protein} = AX_{\alpha-helical} + BX_{\beta-sheet} + CX_{random} \qquad (7)$$

X represents the relative content of the particular secondary structure element, while *A, B* and *C* are the data points of the corresponding basis spectra at a certain wavelength. This means the CD spectrum of a complex protein can be deconvoluted as sum of their particular components. Approaches utilizing this fact for the circular dichroism based

analysis of protein structures have recently been reviewed.[172] Nevertheless, the informational content of deconvolution strategies has to be questioned, since most of the underlying basis spectra are obtained from huge globular proteins and can therefore hardly only be applied for smaller peptide systems. Additionally, the protein conformation needs to be determined accurately, which is inherently an challenging issue. Thus, the accuracy of such strategies is highly restricted. Despite all these pitfalls, CD spectroscopy provides a powerful tool to follow conformational transitions. Especially the structural transition from α-helix/random coil to β-sheet which usually occurs during the process of amyloid formation, can be easily monitored qualitatively by circular dichroism.

4.2 Dye Binding Studies

Dye binding strategies have been used as a diagnostic tool to identify amyloid fibrils in tissues for more than 150 years and are still one of the most common techniques applied on a routine basis. In the very first study, Virchow used iodine to stain abnormal deposits derived from brain tissue and found a starch-like behavior (see section 2). Later, the dye Congo red (CR) was found to exhibit a characteristic apple green birefringence under polarized light, upon binding to amyloids.[20,173] Figure 4.3 A shows the structure of CR.
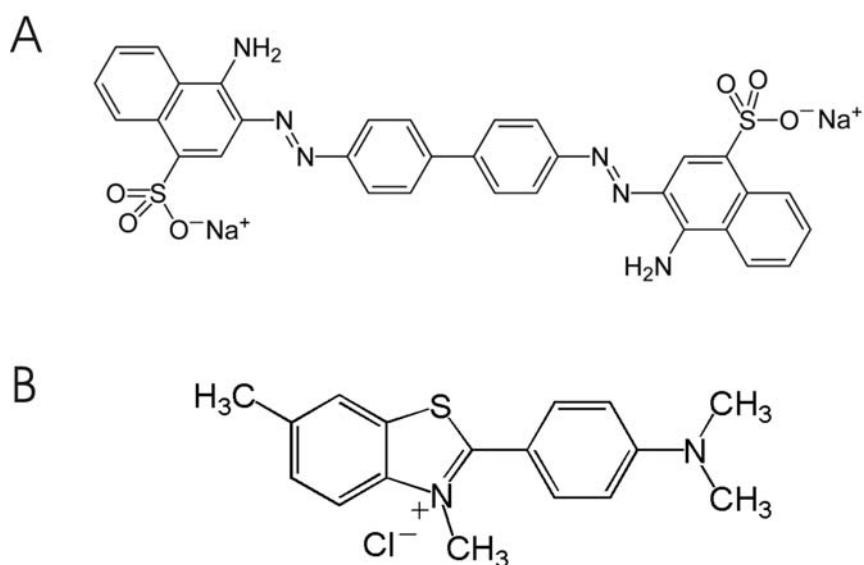
Figure 4.3. Structure of amyloid binding dyes. (A) Congo red, (B) Thioflavin T.

The binding of Congo red to amyloids has been widely used for histological purposes and has, therefore, evolved to a common characteristic of amyloids (see section 2). However, although many attempts highlighted the importance of hydrophobic interactions between β-sheet side chains and CR, the binding specificity and the underlying mechanisms remain unclear.[174,175] Moreover, CR has been shown to act as amyloid inhibitor and may therefore tamper the observed processes.[83,174,176] In addition, the use of CR for the *in vitro* characterization of amyloids is highly restricted to a slight red-shift in the dye's UV spectrum and the induction of a weak signal in circular dichroism[175], which yields merely qualitative information on the amyloid association process. Due to these pitfalls, easier and more reliable staining methods utilizing the high binding affinity of the dye thioflavin T (ThT) have recently emerged. Figure 4.3 B shows the structure of ThT.

Unlike CR, the benefit and convenience of ThT is the ability to gain quantitative information on the amyloid association process. This is based on the fact that ThT, once bound to fibrils, exhibits a large shift in its absorption spectrum and, if excited at λ_{ex} = 450nm, a fluorescence emission at 485nm. The fluorescence emission intensity strongly depends on the amount of aggregated amyloid, and can therefore be utilized to monitor the transition from the native form to aggregated fibrils. Figure 4.4 shows the absorption (A) and emission (B) spectra of ThT in the absence of amyloids and in presence of aggregated $A\beta_{(1-28)}$ and $A\beta_{(1-40)}$.[177]
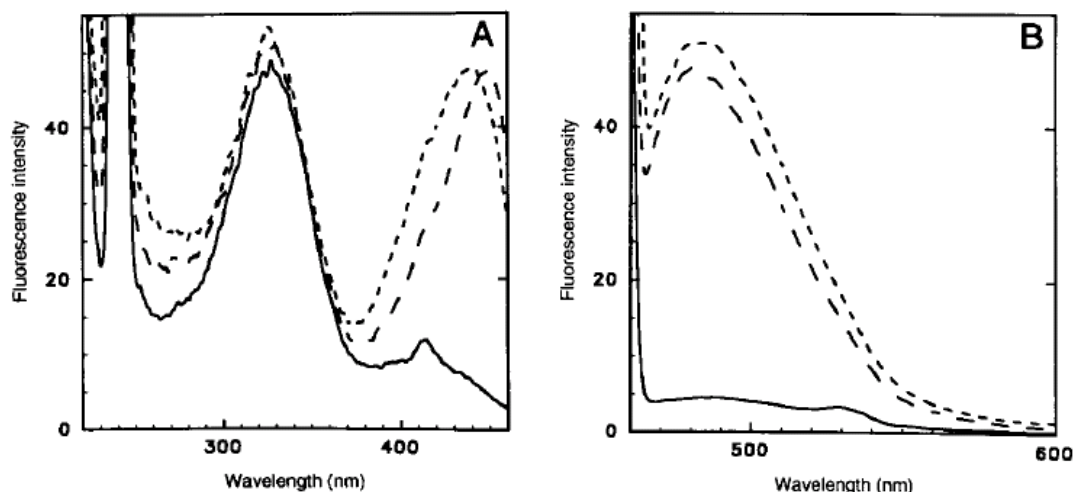
Figure 4.4. *Fluorescence spectra of thioflavin T in the absence (solid line) and in the presence of aggregated $A\beta_{(1-28)}$ (short dashed line) and $A\beta_{(1-40)}$ (long dashed line). (A) Excitation spectra, i.e., absorption. (B) emission spectra at λ_{ex}=450nm (according to H. LeVine, III et al.)[177]*

59

Today, measuring the characteristic ThT fluorescence at certain time points is probably the most widely used approach to follow fibril formation kinetics. For a nucleation dependent growth, a sigmoidal increase of the dyes fluorescence intensity is usually observed. Strategies imaging the fibril growth directly by total internal reflection microscopy have also been reported.[178] In addition, ThT staining assays are very commonly used to study the impact of potential amyloid inhibitors.

The mechanisms leading to the induced fluorescence of ThT in the presence of amyloids is still unclear. Several possibilities have been proposed. Khurana et al. assumed from their experiments that ThT micelles, which have yet been characterized in solution, bind to amyloids as intact units.[179] In contrast, Donald and co-workers suggested a model with dye molecules interdigitated in "channels" between the side chains, parallel to the fibril axis and perpendicular to the β-strands.[180] Figure 4.5 shows a schematic description of this model.[180] Steric interactions between the side chain residues could serve as an explanation for the high specificity but differing efficiency of the ThT-amyloid binding.
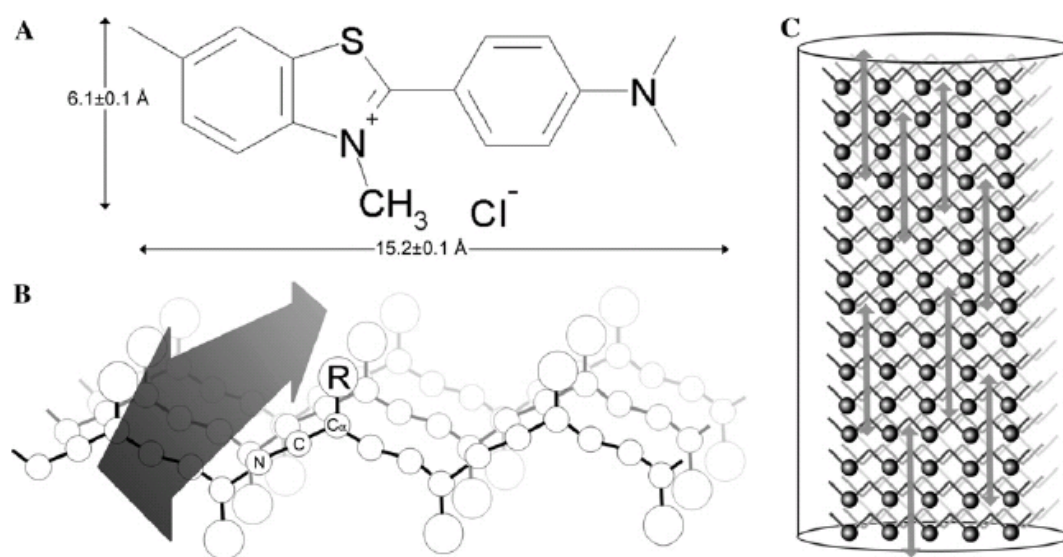
Figure 4.5. *Thioflavin-T and diagram of a β-sheet. (A) Structure and dimensions of thioflavin-T The molecule is 4.3 ± 0.1Å thick. (B) A schematic representation of a β-sheet. Indicated are the backbone atoms (N, C, and C_α) and the side chain (R) for one residue. One of the binding channels is indicated with a double headed arrow. It is thought thioflavin-T binds with its long axis parallel to the long axis of this arrow. (C) Schematic representation of a protofilament with bound ThT molecules represented by double headed arrows (according to M.R.H. Krebs et al.)[180]*

A certain drawback using the ThT staining technique also has to be taken into account because of their aromatic and hydrophobic character. Dyes like ThT and CR tend to form aggregates. These aggregates may nucleate the amyloid association process.[179] Monitoring the time course of fibril formation, therefore, requires the preparation of individual dye containing samples at every time point. Thus, the application of ThT staining assays on a huge scale is highly restricted in terms of sample consumption.
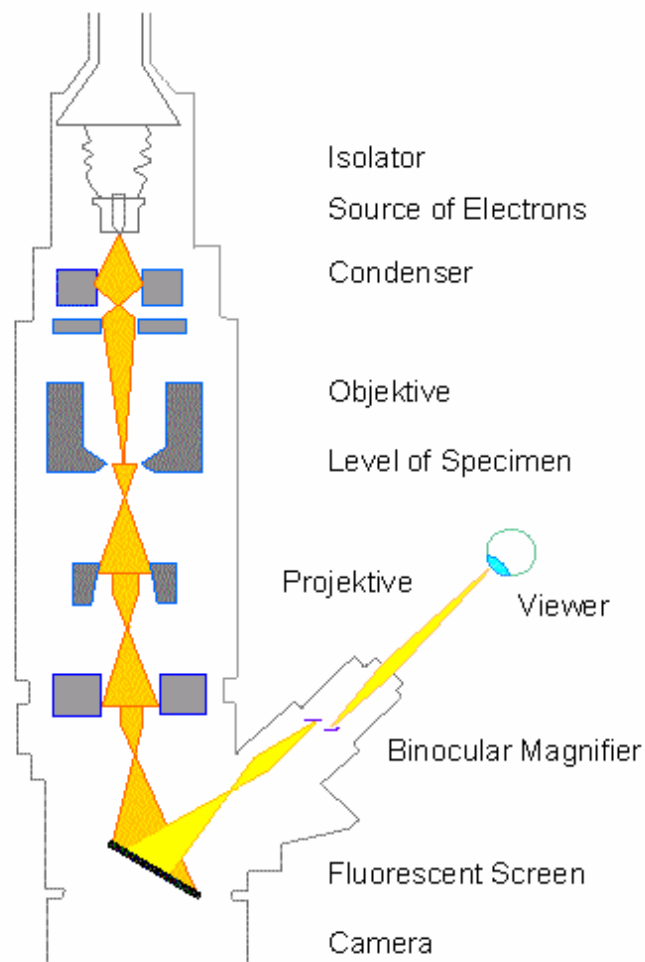
4.3 Transmission Electron Microscopy (TEM)

Macromolecules and their complexes are usually too small to be directly observed by optical microscopy, because their size is insufficient to diffract light of wavelengths in the visible region of the electromagnetic spectrum ($\lambda > 400nm$). The resolving power of conventional light microscopes is narrowed down to approx. $0.2\mu m$ by Abbe's equation. Although modern methods utilizing self-luminous particles such as stimulated emission depletion microscopy (STED) offer an improved resolution of about 15nm[181-183], microscopic techniques applying visible light are usually inapplicable for the characterization of the amyloid fibril morphology.

In contrast to visible light, electron beams can possess up to a 100,000-fold shorter wavelength of a few picometers, e.g., 4.9pm at 60kV.[184] Since particle beams obey the wave-particle dualism introduced by Luis de Broglie, they can be utilized as a radiation source for microscopic techniques. In the last 70 years, this idea yielded a battery of imaging techniques which commonly merged in electron microscopy.[184] The first prototype instrument, a so-called transmission electron microscope (TEM), was developed in 1931 by the german engineer Ernst Ruska and honored with the Noble Prize in physics in 1986.[185] The first commercially available instrument was introduced in 1939 by Siemens. To date, TEM is one of the most powerful microscopy techniques for the visualization and characterization of amyloids. Per definition, amyloid fibers possess characteristic dimensions and exhibit an unbranched morphology (see section 2). Macroscopic structural features of both, *in vivo* and *in vitro* derived samples, are investigated by EM on a routine basis.[23] During the work on this thesis, transmission electron microscopy was used for the characterization of selected model peptide aggregates. Thus, the underlying work principle and certain aspects of sample preparation will be summarized briefly in the following subsections.

4.3.1 Instrumentation

The theory of electron-optics shows that it is possible to build electron-optical counter-parts for most of the optical elements known from conventional light microscopy. Therefore, the set-up of a transition electron microscope is quite similar to that of optical microscopes, which contain lenses that focus a beam on a specimen. Figure 4.6 shows the principle instrumentation of a transmission electron microscope.[186]

Figure 4.6. Schematic representation of a transmission electron microscope (TEM). The electron beam is highlighted in yellow while electron-optical lenses are depicted in grey. Since accelerated electrons possess a very short cross-section, high vaccum (10^{-8} Torr) is required within the instrument (according to P. v. Sengbusch et al.)[186]

TEM represents the original form of all electron microscopy techniques. It involves a high voltage electron beam (~100kV) which is derived by cathode emission. This beam is focused by electrostatic and electromagnetic lenses (condenser system) and transmitted through a specimen that, depending on the spatial amount of staining reagent (negative staining TEM) or sample embedded in vitreous ice (cryo-TEM), is partially transparent to electrons. Consequently, the electron beam carries information about the structure of the specimen and is subsequently transferred to the imaging system of the microscope. There, the image is magnified by a series of electromagnetic lenses (projective system) until it is recorded by hitting a fluorescent screen, photographic plate, or light sensitive sensor such as a CCD (charge-coupled device) camera.

However, spherical aberrations decrease the TEM resolution to a twenty fold of the applied wavelength. Additionally, in reality the instrument setup is subject to many difficulties which makes TEM instruments expensive to buy and maintain. One major disadvantage is the necessity for high vacuum conditions (10^{-8} Torr). This can be explained by the nature of particle beams in general. Accelerated particles, such as electrons, possess a very small cross section, i.e., a short free path length. In other words, there is a high probability that the particle beam collides with free gas molecules in the instrument. These collisions result in a variety of elastic and inelastic scattering events yielding an electron beam that is fairly heterogeneous in terms of wavelength and energy. Thus, high vacuum conditions are needed to minimize the disturbing effects of gas molecules. Therefore, the instrument is equipped with a pre-vacuum, a diffusion, and several ion-getter pumps which are continuously in operation. Extremely stable high-voltage supplies for the electron acceleration and stable currents to each electromagnetic coil/lens are also necessary. Such requirements are demanding in terms of instrument design and operation, even if state-of-the-art electronics are applied.

Beside TEM, several other microscopic methods with distinctly different working principle utilize electron beams, two of which should at least be mentioned. Scanning electron microscopy (SEM), for example, produces images by detecting low energy secondary electrons which are emitted from the surface of the specimen due to excitation by the primary electron beam. The image arises from the detection of secondary electron signals while the beam is rastered across the sample. Reflection Electron Microscopy (REM) is widely used for the characterization of biological tissues or entire micro organisms. Like TEM, this technique involves electron beams that are accelerated onto a

surface but instead of using its transmission (TEM) or the generation of secondary electrons (SEM) the reflected beam is detected.

4.3.2 Formation of Contrast

One of the biggest challenges in TEM is the generation of contrast. Since electron beams have a very different wavelength compared to visible light, they certainly show distinctive interactions with matter. When an electron beam strikes an object, several things may happen: (a) If the electron does not strike an atom in the sample, it will continue to travel in a straight line until it hits the imaging screen. If the electron gets in contact with the sample, it can either (b) bounce off elastically, without any loss of energy, or (c) inelastically (because of interactions with the electrons of the object) transferring some of its energy to the atom. If the electron is bounced elastically (usually by Coulomb interactions with the nucleus of the object), its energy is constant, and the law of conservation of momentum will determine the angle at which it will bounce. This effect is used for electron diffraction experiments. Electrons with a scattering angle above 90° are termed "back reflected electrons" and are used generally not in electron microscopy. The residual amount of energy carried by the electron, on the other hand, is random after an inelastic bounce (usually because of interactions with the electrons of the object). When the electron reaches the imaging plane, if at all, it has an unknown energy and angle and, as a result, yields noise. As a side effect, transfer of the electron's energy to the sample causes radiation damages which decrease resolution. However, inelastically scattered electrons carry information about the element composition of the object which is used for spectroscopy and imaging methods such as electron energy loss spectroscopy (EELS) and electron spectroscopic imaging (ESI). Details can be obtained from the literature.[187]

Negative Staining TEM

In conventional TEM elastical scattering effects are mainly used for the generation of a transmission contrast. Biological samples inherently show very weak electron scattering, since they are usually composed of low-weight atoms such as C, H, N, O, and S. In comparison to this, heavy metal atoms such as lead, gold and uranium possess a much higher radius, weight, and charge of the nucleus. If bounced by accelerated electrons, heavy metal ions scatter the electron beam vigorously and, as a result, enhance the contrast. Furthermore, higher electron energy can be implemented, since the large

amount of scattering prevents radiation damage of the sample. Coating of biological samples with heavy metal ions is therefore an obvious strategy for the generation of contrast. Two general approaches have prevailed for practical use. Frozen biological tissues and cells with a comparatively huge cross section can be sputtered with metal atoms directly. Afterwards, the coated surfaced is stabilized by carbon-sputtering and the biological material is removed by oxidizing reagents. The literature has further information regarding this technique.[187] For the visualization of proteins and protein complexes, negative staining TEM emerged as one of the most powerful techniques.[188] Since it is an easy and rapid method, it enables a characterization of amyloids on a routine basis with resolutions up to 1nm.[187] Therefore, the generation of a reverse contrast by immersion of the sample into a heavy metal ion solution is applied. Figure 4.7 A shows the sample cross section and the resulting image profile.[187]

In practice, aqueous solutions or precipitates of proteins are deposited on a carbon coated grid and adsorbed for approximately one minute. Remaining moisture is discarded by soaking with filter paper. Subsequently, the sample is covered with a droplet of an appropriate staining reagent solution. After a few seconds the drop is blotted dry and the sample is ready for viewing. A list of capable staining reagents covering a huge range of pH and radiation conditions is shown elsewhere.[187] During the measurement, the contrast arises from scattering of the electron beam at the staining reagent which is deposited depending on the spatial adjacency of sample. In other words, the amount of heavy metal ions but not the sample itself generates the image which therefore yields an inverted, negative picture of the sample profile (Figure 4.7A). The usually huge resistance of the staining reagent towards the electron beam is adventurous, since higher beam intensities can be applied. However, there are some drawbacks, namely, the sample particles usually loose their hydration shell during the drying process. Since this hydration often stabilizes the conformation, distortions of the particle shape may occur. Additionally, uneven stain depositions, often referred to as artifacts, may occur depending on the particle shape. As a result, certain areas might acquire more stain and therefore appear with higher contrast than would be normal. Nevertheless, since negative staining TEM is not very demanding in terms of sample preparation it represents a routinely used method for the characterization of amyloids.
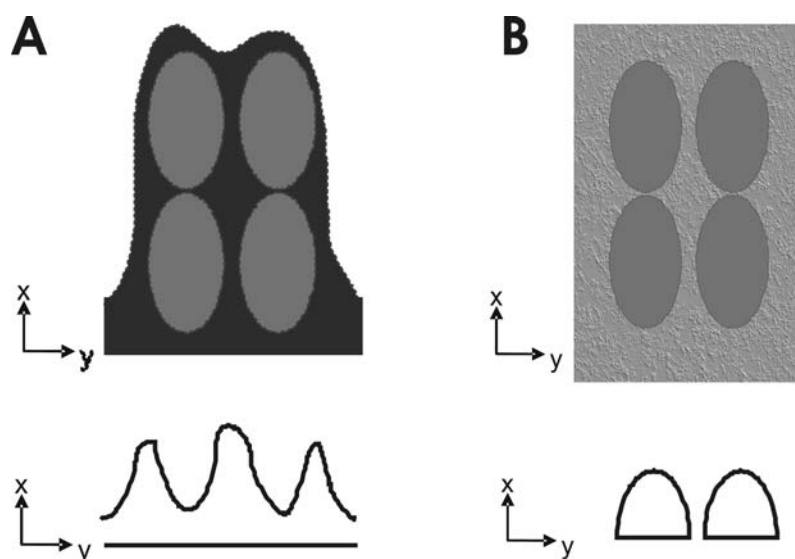
Figure 4.7. *Origin of contrast in (A) negative staining TEM and (B) cryo TEM. The specimen (top) are transmitted by an electron beam yielding a density profile (down). Negative staining results in an inverted picture of the sample since the contrast is mainly achieved from interactions between beam and staining reagent (A, black). In contrast, cryo TEM yields a positive picture of the specimen. Here the contrast is generated by weak interactions between electron beam and the ice-embedded sample (B, grey circles) (according to Lottspeich et al.)[187]*

Cryo-TEM

However, negative staining only provides a picture of the outer sample structure. To gain information on the inner core of biological molecules and aggregates, it is mandatory to work in the absence on contrast reagents. Cryo-TEM emerged as the most powerful technique to tackle this claim.[189] As indicated by the term "cryo," frozen samples are used to ensure immobilization and a consecutive structural conservation of the biological molecules which can be obtained directly from native-like, aqueous solutions. The crucial factor is the process of freezing. Conventional cubic ice is ineligible since it would absorb the electron beam. If the sample freezing is quick enough, though the water can be solidified as an amorphous solid (vitreous ice) containing randomly ordered water molecules. As a result of the poor degree of ordering, vitreous ice is transparent to electron beams and can therefore be employed for TEM applications. However, the scattering of the electron beam is purely generated by vitrified biomolecules and therefore yields a positive image profile (Figure 4.7 B). Thus, the contrast is very low since biological molecules usually do not contain heavy atoms. Nevertheless, the

image represents a snapshot of the molecular conformation at native conditions and can be used for the reconstruction of three dimensional structures.[25,27] The 3D maps of several insulin fibrils shown in Figure 2.1 have been obtained using this methodology.[25] Unfortunately, it is almost impossible to apply cryo-TEM, especially in combination with 3D structure modeling, on a routine basis. The sample preparation procedures are un-equally more difficult than those of negative staining. The freezing procedure is carried out in liquid ethane and is therefore very demanding. Furthermore, the samples need to be prepared as very thin layer in order to not further repress the already low contrast. Additionally, the specimen needs cooling throughout to avoid melting and evaporation, even after transfer into the instrument. A combination of both, however, the fast and easy negative staining TEM as well as the demanding but meaningful cryo-TEM has an enormous potential to information on the morphology of aggregated proteins.